


RESEARCH ARTICLE

Proteome-minimized outer membrane vesicles from *Escherichia coli* as a generalized vaccine platform

Ilaria Zanella¹ | Enrico König¹  | Michele Tomasi¹ | Assunta Gagliardi¹ |
 Luca Frattini¹ | Laura Fantappiè² | Carmela Irene¹ | Francesca Zerbini¹ |
 Elena Caproni¹ | Samine J. Isaac¹ | Martina Grigolato¹ | Riccardo Corbellari¹ |
 Silvia Valensin² | Ilaria Ferlenghi³ | Fabiola Giusti³ | Luca Bini⁴ | Yaqoub Ashhab⁵ |
 Alberto Grandi^{2,6} | Guido Grandi¹

¹ Department of Cellular, Computational and Integrative Biology (CIBIO), Laboratory of Synthetic and Structural Vaccinology, University of Trento, Trento, Italy

² Toscana Life Sciences Foundation, Siena, Italy

³ GlaxoSmithKline Vaccines, Siena, Italy

⁴ Department of Life Sciences, Functional Proteomics Laboratories, University of Siena, Siena, Italy

⁵ Palestine-Korea Biotechnology Center, Palestine Polytechnic University, Hebron, Palestine

⁶ BiOMViS Srl, Siena, Italy

Correspondence

Prof. Guido Grandi, CIBIO, University of Trento,
 Via Sommarive, 9, 38123 Trento, Italy.
 Email: guido.grandi@unitn.it

Current address

Francesca Zerbini, Medimmune/Astra Zeneca,
 Granta Park, CB21 6GP, Cambridge, UK.

Ilaria Zanella and Enrico König contributed equally
 to this study.

Funding information

Advanced European Research Council,
 Grant/Award Number: OMVAC 340915; National
 Funding PRIN-2015, Grant/Award Number:
 CUPE62F16001630001

Abstract

Because of their potent adjuvanticity, ease of manipulation and simplicity of production Gram-negative Outer Membrane Vesicles OMVs have the potential to become a highly effective vaccine platform. However, some optimization is required, including the reduction of the number of endogenous proteins, the increase of the loading capacity with respect to heterologous antigens, the enhancement of productivity in terms of number of vesicles per culture volume. In this work we describe the use of Synthetic Biology to create *Escherichia coli* BL21(DE3) Δ 60, a strain releasing OMVs (OMVs $_{\Delta$ 60) deprived of 59 endogenous proteins. The strain produces large quantities of vesicles (> 40 mg/L under laboratory conditions), which can accommodate recombinant proteins to a level ranging from 5% to 30% of total OMV proteins. Moreover, also thanks to the absence of immune responses toward the inactivated endogenous proteins, OMVs $_{\Delta$ 60 decorated with heterologous antigens/epitopes elicit elevated antigens/epitopes-specific antibody titers and high frequencies of epitope-specific IFN- γ -producing CD8⁺ T cells. Altogether, we believe that *E. coli* BL21(DE3) Δ 60 have the potential to become a workhorse factory for novel OMV-based vaccines.

KEYWORDS

cancer, infectious diseases, outer membrane vesicles (OMVs), synthetic biology, vaccines

1 | INTRODUCTION

More than 60 years ago, it was accidentally discovered that Gram-negative bacteria release Outer Membrane Vesicles (OMVs) (Bishop & Work, 1965; Chatterjee & Das, 1967). As often happened in science, the discovery remained almost unnoticed for

This is an open access article under the terms of the [Creative Commons Attribution](https://creativecommons.org/licenses/by/4.0/) License, which permits use, distribution and reproduction in any medium, provided the original work is properly cited.

© 2021 The Authors. *Journal of Extracellular Vesicles* published by Wiley Periodicals, LLC on behalf of the International Society for Extracellular Vesicles

several years and only recently, scientists became aware of the amazing aspects of the OMV biology and of their potential for biotechnological applications. OMVs are closed spheroid particles of heterogeneous size, 50–300 nm in diameter, generated through a ‘budding out’ of the bacterial outer membrane. They represent a distinct secretory pathway with a multitude of functions, including inter and intra species cell-to-cell cross-talk, biofilm formation, genetic transformation, defence against host immune responses, and toxin and virulence factor delivery to host cells (Ellis & Kuehn, 2010; Kulp & Kuehn, 2010).

OMVs are becoming an attractive vaccine platform for their excellent adjuvanticity (Chen et al., 2010; Ellis & Kuehn, 2010), the possibility of decorating them with heterologous antigens (Gerritzen et al., 2017; Irene et al., 2019; Kesty & Kuehn, 2004), and the simplicity of their production and purification process (Berlanda Scorza et al., 2012). Indeed, OMV-based vaccines have already reached the market (Ladhani et al., 2016; Serruto et al., 2012), while others are in advanced clinical phases (Gerke et al., 2015; Rossi et al., 2016).

OMV-based vaccines can be classified in two categories. The first one includes vaccines constituted by OMVs directly purified from the pathogen of interest (Kaparakis-Liaskos & Ferrero, 2015; Van Der Pol et al., 2015). The rationale of developing such vaccines is that OMVs provide both the immune stimulatory molecules (adjuvants) and the protective antigens. The prototype of this category is Bexsero, the Meningococcal Group B vaccine, which, in addition to purified meningococcal antigens, is formulated with vesicles from the *Neisseria meningitidis* New Zealand strain (Parikh et al., 2016). The second category includes OMVs decorated with heterologous antigens and obtained from a properly engineered Gram-negative bacterial species (Kaparakis-Liaskos & Ferrero, 2015; Van Der Pol et al., 2015). Such vaccines exploit the excellent adjuvanticity properties of OMVs and have the advantage to potentially target any kind of bacteria, viruses and cancer, provided that specific protective antigens are selected.

No vaccines belonging to the second category are currently available for humans. This is in part because for its full-blown development, the OMV platform still needs to be optimized. Such optimization should include the development of efficient strategies for OMV engineering, the modulation of the OMV adjuvanticity to avoid potential reactogenicity, and the elimination of unnecessary OMV endogenous proteins.

Here, we describe the application of Synthetic Biology for the construction of a novel *E. coli* strain, named *E. coli* BL21(DE3) Δ 60, releasing OMVs (OMVs $_{\Delta$ 60) deprived of 59 endogenous proteins. The rationale for creating such strain is threefold. First, we hypothesized that by eliminating OMV endogenous proteins we could increase the loading capacity of OMVs with respect to recombinant antigens. Second, we predicted that heterologous antigens expressed in proteome-minimized OMVs should be more immunogenic because of their increased amount in OMVs and of the absence of endogenous proteins that could dilute the antigen-specific immune responses. Third, in view of human applications, the availability of OMVs carrying a reduced number of irrelevant proteins should offer an important additional advantage. As predicted, we show that OMVs $_{\Delta$ 60 have a number of important features, which ultimately lead to the elicitation of potent antibodies and T cell responses against heterologous antigens. Overall, our data indicate that *E. coli* BL21(DE3) Δ 60 is a particularly useful strain for the development of effective vaccines against infectious diseases and cancer.

2 | MATERIALS AND METHODS

2.1 | Bioinformatics analysis and software

The *E. coli* BL21(DE3) proteome was analyzed to predict membrane-associated and periplasmic proteins. A meta-prediction pipeline that employs different subcellular localization prediction tools in three phases of positive and negative selections was used (Hisham & Ashhab, 2018). The identified proteins were subsequently assessed for their biological function and classified (essential vs. non-essential) according to the ‘Keio collection’ (Baba et al., 2006), and EcoCyc *E. coli* database (Keseler et al., 2017), respectively. Oligonucleotides for guide DNAs, donor DNAs and primers were designed using Serial Cloner and Benchlink and BLAST was used for alignments (Altschul et al., 1990). Densitometry was performed with Image Studio Lite Version 5.2 (Li-Cor Biosciences, Lincoln, NE USA) and for 2-DE map analysis, ImageMaster 2D Platinum v.6.0 software was used (GE Healthcare, Chicago, IL USA).

2.2 | Bacterial strains, culture conditions and plasmids

E. coli strains (BL21(DE3) derivatives, DH5 α , TOP10) were routinely cultured in lysogeny broth (LB Miller; Merck, Darmstadt, Germany) supplemented with 100 mg/L ampicillin (Carl Roth, Karlsruhe, Germany), 25 mg/L chloramphenicol (Merck, Darmstadt, Germany), 50 mg/L kanamycin (Thermo Fisher Scientific, Waltham, MA USA) or a combination of them, where necessary. For recombinant protein expression in OMVs, cultures were supplemented with 0.1 mM isopropyl- β -D-thiogalactopyranoside (IPTG, Merck, Darmstadt, Germany) at OD₆₀₀ between 0.5 and 0.7 and OMVs were collected after 4 h from induction. Fermentation was carried out in an EZ control bioreactor (Applikon Biotechnology, Schiedam, Netherlands) at 30°C until OD₆₀₀ 0.5,

then growth continued at 25°C, pH 6.8 (± 0.2), dO₂ > 30%, 280–500 rpm. At OD₆₀₀ 1.0, the culture was induced with 0.1 mM IPTG together with a feed consisting in ampicillin (50 mg/L) or chloramphenicol (12.5 mg/L), glycerol (15 g/L), and MgSO₄ (0.25 g/L).

Plasmids encoding FhuD2, SpA_{KKAA}, CsaI, Hla_{H35L}, FhuD2-mFAT1 and Nm-NHBA were already described (Fantappiè et al., 2017; Grandi et al., 2018; Irene et al., 2019). For the construction of plasmids encoding ClfA_{Y338A}, FhuD2-Bp, FhuD2-OVA and FhuD2-hFAT1, the PIPE-PCR method was used (Klock & Lesley, 2009). Briefly, the coding sequences were chemically synthesized (Geneart, Thermo Fisher Scientific, Waltham, MA USA) and PCR amplified or several oligonucleotides were assembled stepwise (in case of Bp) using the primers reported in Table S3. In parallel, a pET21b+ derivatives carrying either the sequence encoding the leader peptide for secretion of *E. coli* Lpp (pET-Lpp plasmid) or Lpp-FhuD2 (for epitope fusions) (Irene et al., 2019) were linearized using the primer couples Lpp-R-plasmid/nohisflag and Lpp-FhuD2-R-plasmid/nohisflag, respectively (Table S3). The PCR products were digested with DpnI (New England Biolabs, Ipswich, MA USA), combined (2 μ L each) and used to transform *E. coli* HK100 chemically competent cells. Positive clones identified by colony PCR using GoTaq Green Master Mix (Promega, Madison, WI USA) and gene specific primer (Table S3) were subjected to sequence analysis (Eurofins Scientific, Luxemburg) before using the resultant plasmids (Table S3) for transformation of OMV producer strains.

2.3 | Construction of *E. coli* BL21(DE3) Δ 60

Gene deletions were accomplished using our previously established CRISPR/Cas9-based genome editing protocol (Zerbini et al., 2017). The preparation of the 90 pCRISPR-SacB-gDNA plasmids were done using double-stranded synthetic oligonucleotides (Merck, Darmstadt, Germany) encoding for the guide RNA reported in Table S4. Stepwise single gene mutagenesis was achieved by co-transformation of electrocompetent cells of the recipient strain (*E. coli* BL21(DE3) Δ ompA_pCasRed, *E. coli* Δ 01_pCasRed, etc.) with the gene-specific pCRISPR-SacB-gDNA and its respective double-stranded donor DNA (ds-dDNA) (Table S5). Gene-specific primer pairs used for screening of colonies with GoTaq Green Master Mix (Promega, Madison, WI USA) are listed in Table S6. Genomic DNA was extracted from *E. coli* BL21(DE3) Δ ompA and *E. coli* BL21(DE3) Δ 58 using PowerSoil DNA Isolation Kit (Mo Bio Laboratories, Carlsbad, CA USA) and the genomes were fully sequenced. Briefly, libraries were prepared using the Nextera XT DNA Library Preparation Kit (Illumina, San Diego, CA USA), and library quality was assessed using the Caliper LabChip GX (High-Throughput Bioanalyzer) following manufacturers guidelines. Sequencing was performed on the HiSeq 2500 system (Illumina, San Diego, CA USA).

2.4 | Expression and purification of recombinant proteins

FhuD2 and Hla_{H35L} *S. aureus* proteins were purified as previously described (Irene et al., 2019). The genes encoding the *E. coli* BL21 proteins Agp, CpoB, EfeO, FepA, GlpQ, LamB, MalE, MalM, OppA, Pal, YdcL and YncD were amplified from chromosomal DNA and cloned as His-TAG C-terminal fusions using linearized pET15+ plasmid using PIPE method (Table S3). Proteins were purified using Ni-NTA resin (Qiagen, Hilden, Germany) following standard purification procedures.

2.5 | OMV purification and electrophoretic analysis

For assessment of OMV productivity of each mutant we used 50 ml culture volume, whereas OMVs for antigen expression analysis and batch preparation for immunization were purified from 200 ml and 1 L cultures, respectively. OMVs were collected from culture supernatants by filtration through a 0.22 μ m pore size filter with a syringe for small volumes up to 50 ml (Merck, Darmstadt, Germany) or with a filter system for larger volumes (Starlab, Hamburg, Germany). Small volumes (50 ml and 200 ml) were applied to high-speed centrifugation (174,900 \times g for 2 h at 4°C) and pellets containing OMVs were resuspended in PBS (Gibco brand, Thermo Fisher Scientific, Waltham, MA USA). Purification of OMVs from cultures in bioreactor was carried out using Tangential Flow Filtration (ÄKTA flux system; GE Healthcare, Chicago, IL USA) with a Hollow Fibre cartridge UFP-500-C-3MA (GE Healthcare, Chicago, IL USA). Protein content of OMVs was quantified using DC Protein Assay (Bio-Rad) and the quality of OMVs was monitored by SDS-PAGE loading OMVs (normalized by μ g) on Any kD Criterion TGX Stain-Free Protein Gel (Bio-Rad Laboratories, Hercules, CA USA) stained using ProBlue Safe Stain (Giotto Biotech, Sesto Fiorentino, Italy). The detailed purification protocol has been submitted to EV-TRACK (ID EV200158).

2-DE was performed as previously reported (Fantappiè et al., 2017; Gagliardi et al., 2016). For analytical and MS-preparative gels, 250 μ g and 500 μ g of protein, respectively, were diluted in 350 μ L of denaturation buffer and 0.2% or 2% (v/v) IPG-buffer (pH 3–10; GE Healthcare, Chicago, IL USA). Analytical gels and MS-preparative gels were stained with ammoniacal silver nitrate and MS-compatible silver staining, respectively, before being scanned using the ImageScanner III (GE Healthcare, Chicago,

IL USA). Image analysis was performed on 2-DE analytical gels using the ImageMaster 2D Platinum v.6.0 software (GE Healthcare, Chicago, IL USA). For each OMV preparation, OMVs _{Δ ompA} and OMVs _{Δ 60}, image analysis was carried out on three different spot maps. Qualitative differences between OMVs _{Δ ompA} and OMVs _{Δ 60} were considered significant only when absence/presence of protein spots was observed in all three corresponding gels.

2.6 | Negative staining electron microscopy method

A volume of 5 μ l of OMV diluted at 80 ng/ μ l in PBS were loaded onto a copper 200-square mesh grid of carbon/formvar rendered hydrophilic by glow discharge using a Q150R S (Quorum, East Sussex, UK). The excess solution was blotted off after 30 s using Whatman filter Paper No.1. The grids were negatively stained with NanoW (Nanoprobes, Yaphank, NY USA) for 30 s, then blotted using Whatman filter Paper No.1 and finally let air dry. Micrographs were acquired using a Tecnai G2 Spirit Transmission Electron Microscope equipped with a CCD 2kx4k camera at a final magnification of 120000x.

2.7 | Protein identification by mass spectrometry

Protein identification was carried out by peptide mass fingerprinting (PMF) using an Ultraflex III MALDI-TOF/TOF mass spectrometer (Bruker Daltonics, Billerica, MA USA), equipped with a 200 Hz smartbeam I laser, as already described (Fantappiè et al., 2017; Gagliardi et al., 2016). Mass spectra were acquired in reflector positive mode with a laser frequency set to 100 Hz. Flex Analysis software v.3.0 was used for analysis. Acquired spectra were internally calibrated using auto-proteolytic trypsin peptides (842.509 m/z and 2,211.105 m/z) and contaminants were removed from the obtained mass lists. PMF searching was carried out against entries for *E. coli* in the SwissProt database using Mascot software (Matrix Science Ltd., London, UK, www.matrixscience.com) with 100 ppm as peptide tolerance, monoisotopic peptide mass, allowing one missed cleavage by trypsin, carbamidomethylation of cysteine as fixed modification, and oxidation of methionine as variable modification. The parameter used to accept identifications was the default Mascot protein score greater than 56, corresponding to a 5% probability that the observed match was a random event ($P < 0.05$). The number of matched peptides and the extent of sequence coverage were also considered to confirm protein identification. Protein spots that emerged as significant qualitative differences along with the MS data for those that were successfully identified by MS are reported in Table S2.

2.8 | Assessment of phospholipid content, particle size and dimension of OMVs

For lipid quantification, styrylic membrane dye FM4-64 (Thermo Fisher Scientific, Waltham, MA USA) at a final concentration of 3.3 μ g/ml was added to 125/250 ng of OMVs (protein content) resuspended in PBS in a black 96-well OptiPlate (Perkin Elmer, Waltham, MA USA). As standard, we used *E. coli* L- α -phosphatidylglycerol (Merck, Darmstadt, Germany) in a range between 5 μ g and 0.15 μ g. The reaction was incubated for 10 min at 37°C and fluorescence (excitation at 485 nm, emission at 670 nm) was measured with an Infinite M200PRO plate reader (Tecan, Männedorf, Switzerland).

Assessment of particle size and dimension on OMVs diluted in PBS to a concentration of 100 ng/ml was performed using a Nanosight NS300 (Malvern Instruments, Malvern, UK) with a 532 nm laser, camera level 15, slider shutter and gain of 1206 and 245, respectively. Three videos of 60 s were recorded and analyzed with the software NTA 3.4 Build 3.4.003.

2.9 | Toll-Like-Receptor agonistic activity and IL-6 stimulation

OMV agonistic activity of human Toll Like Receptor 2 (hTLR2) and mouse Toll Like Receptor 4 (mTLR4) was measured using HEK-Blue™ hTLR2 or HEK-Blue™ mTLR4 Cells, respectively, and QUANTI-Blue (InvivoGen, San Diego, CA USA) as substrate as previously described (Irene et al., 2019). For the IL-6 assay, THP-1 human leukemic monocyte cells were cultured in RPMI 10% FBS and differentiated into macrophages by adding 10 ng/ml of phorbol 12-myristate 13-acetate (PMA) and incubating cells at 37°C 5% CO₂ for 48 h. Then 4×10^5 cells in a volume of 10 μ l/well of RPMI culture medium were aliquoted into a 96 well-plates (Corning, Corning, NY USA). Different concentration of OMVs and purified LPS (control) were added to 90 μ l/well of RPMI in duplicate starting from an initial concentration of 10,000 ng/ml to a final concentration of 10 pg/ml with 10-fold serial dilutions. Cells and OMVs were incubated at 37°C O/N. IL-6 release in supernatants was measured by Human IL-6 Uncoated ELISA™ Kit (Thermo Fisher Scientific, Waltham, MA USA). Corning Costar ELISA plates were coated with 100 μ L/well of anti-human IL-6 antibodies and incubated at 4°C O/N. The day after 100 μ L/well of cell supernatants were transferred to the plate and incubated 2 h at room temperature (RT) and the assay was completed following the manufacturer's protocol. Plates were read at 450 nm using a SpectraMax M2 Microplate reader (Molecular Devices, San José, CA USA).

2.10 | Animal experiments

All mice were purchased from Charles River Laboratories (Wilmington, MA USA). Animal experiments were carried out in accordance with experimental protocols reviewed and approved by the Animal Ethical Committees of University of Trento (Trento, Italy) and Toscana Life Sciences (Siena, Italy) and by the Italian Ministry of Health. Animal health was evaluated using a 0 (no signs of stress and suffering) to 6 (severe signs of stress and suffering) 'pain score' scale approved by the Animal Welfare Committees of University of Trento and Toscana Life Sciences in accordance with the 'Working document on a severity assessment framework - National Competent Authorities for the implementation of Directive 2010/63/EU on the protection of animals used for scientific purposes'. The evaluation considers the recommendations of the Federation of European Laboratory Animal Science Associations (FELASA) (Baumans et al., 1994). This 'pain score' scale is based on objective parameters and are assigned as follows: score 0: normal hair, mucosa, physical activity and nourishment; score 1: ruffled hair coat (piloerection), lesions or dehydration; score 2: as in 1 and reduced physical activity (e.g., grooming, exploration); score 3: as in 2 and lethargy and loose < 10% body weight; score 4: as in 3 and signs of respiratory impairment (dyspnoea or tachypnea); score 5: as in 4 and loss of body weight between 10% and 20%, lordosis or kyphosis; score 6: as in 5 and body weight loss > 20% (animals have to be sacrificed). For antibody titers, female BALB/c mice (5 per group) were immunized intraperitoneally (i.p.) on days 0, 14 and 28 with 2 μ g of OMVs in the presence of Alum (2 mg/ml). Blood was collected by cardiac puncture from euthanized mice at day 35 and serum was obtained from blood through centrifugation at 2,000 rpm for 10 min. For T cell analysis, C57BL/6 mice were subcutaneously (s.c.) injected on days 0 and 7 with 10 μ g of OMVs $_{\Delta 60}$ + 5 μ g of either OVA or SV40 synthetic peptides. At day 12, spleens were collected and used to perform intracellular cytokine staining for subsequent analysis.

2.11 | Analysis of OMV immunogenicity by western blot and ELISA

Purified recombinant *E. coli* proteins (1 μ g each) or total OMV proteins (10 μ g) were loaded on Any kD Criterion TGX Stain-Free Protein Gel (Bio-Rad, Laboratories, Hercules, CA USA) and then transferred onto a nitrocellulose membrane using iBlot transfer stack (Thermo Fisher Scientific, Waltham, MA USA). Sera from mice immunized with OMVs $_{\Delta ompA}$ and OMVs $_{\Delta 60}$ were used at 1:1,000 dilutions and immunogenic proteins were detected with anti-mouse IgG-HRP antibodies (Agilent, Santa Clara, CA USA) at a dilution of 1:2,000 using ECL Select Western Blotting Detection Reagent (GE Healthcare, Chicago, IL USA).

Antigen specific antibody titers elicited by engineered OMVs were measured by ELISA as previously described (Irene et al., 2019) using FhuD2, Hla_{H35L}, *Burkholderia pseudomallei* flagellin epitope (Bp) as recombinant proteins and D8-FAT peptide (IQVEATDKDLGPNHGHTYSIVTDTD; Genscript Biotech, Piscataway Township, NJ USA) (200 ng each).

2.12 | HLA neutralization assay

HLA neutralization assay was performed as previously described (Irene et al., 2019).

2.13 | Analysis of OVA and SV40-specific T cells

Percentage of OVA- and SV40-specific T cells in immunized mice was performed as previously described (Grandi et al., 2018). Statistical significance was assessed using two-tailed Student's *t*-test.

3 | RESULTS

3.1 | Selection of endogenous proteins to be eliminated from *E. coli*-derived OMVs

With the final goal to create an *E. coli* derivative releasing 'proteome-minimized' OMVs, we first experimentally defined the proteome of OMVs from the hypervesiculating strain *E. coli* BL21(DE3) $\Delta ompA$ by using two-dimensional gel electrophoresis (2-DE) coupled to mass spectrometry analysis (MS) as described in Fantappiè et al (Fantappiè et al., 2017). A total of 128 sequences were identified corresponding to 81 unique *E. coli* proteins. 2-DE-MS was coupled to bioinformatics analysis of the *E. coli* BL21(DE3) genome aimed at predicting all periplasmic and outer membrane proteins. We selected 504 proteins, which included all the 81 proteins identified by MS. Next, from these 504 proteins we excluded those ones that were classified as "indispensable" according to the Keio library (Baba et al., 2006), and we finally generated a priority list of 90 proteins, 63 of which identified by MS on 2D map, to be eliminated from our progenitor strain *E. coli* BL21(DE3) $\Delta ompA$ (Table S1).

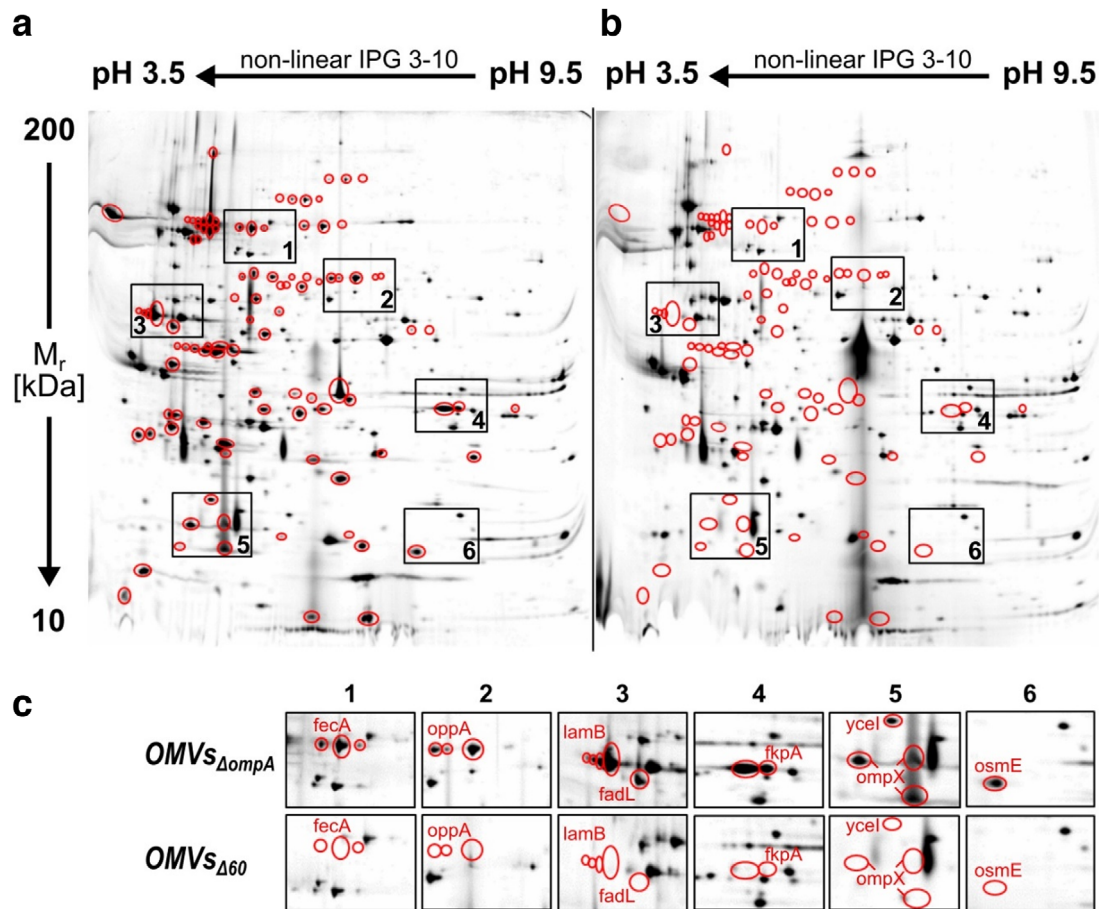


FIGURE 2 Comparison of two-dimensional electrophoresis of OMVs_{ΔompA} and OMVs_{Δ60} - Silver stained 2-DE gels of OMVs from *E. coli* BL21(DE3)ΔompA (a) and *E. coli* BL21(DE3)Δ60 (b). Red circles visualize those protein spots visible in OMVs_{ΔompA} and not visible in OMVs_{Δ60}. All spots not present in OMVs_{Δ60} were removed from the OMVs_{ΔompA} gel, digested with trypsin and analyzed by mass spectrometry. Zoom areas (c) are taken as examples of qualitative differences between the two gels and report the ID of the MS-identified proteins (see Table S1 for annotations)

potential reactivity of LPS-associated OMVs, the genome editing process was completed with the addition of *msbB* and *pagP* gene inactivation, which results in the synthesis of a penta-acylated Lipid A (Somerville et al., 1996; Vorachek-Warren et al., 2002). The final strain, carrying a total of 60 gene deletions, was named *E. coli* BL21(DE3)Δ60.

The correctness of each gene inactivation was first verified by PCR and sequence analyses using primers spanning the mutated regions (Fig. S1) and subsequently by sequencing of the whole genome that has been deposited at GenBank under the accession JADXDS000000000. Moreover, the disappearance from the vesicular compartment of the proteins encoded by the deleted genes was followed by comparing the 2D map of OMVs_{Δ60} and OMVs_{ΔompA}. A total of 98 protein spots were no longer visible in the 2-DE map of OMVs_{Δ60} (Figure 2). Of these 98 spots, 75 were successfully identified in OMVs_{ΔompA} 2-DE map by MS analysis, and they corresponded to 46 unique proteins, 43 of which encoded by the deleted genes (Table S2 and Fig. S2). The disappearance of three proteins not encoded by the deleted genes (Table S1) could be ascribed to the fact that their expression level, which was already low in OMVs_{ΔompA}, could be further reduced by the inactivation of other genes. As far as the remaining 16 out of the 59 inactivated proteins are concerned, two are MsbB and PagP and the other 14 belong to the group of proteins that were selected by bioinformatics analysis. From the 2D map analysis of OMVs_{Δ60} the disappearance of the 59 proteins did not correspond to a substantial increase of specific protein spots. The stained material that appeared at the centre of the 2D gel probably represents a technical artefact since it does not carry proteinaceous material, as judged by mass spectrometry analysis.

3.3 | Properties of *E. coli* BL21(DE3)Δ60 and OMVs_{Δ60}

Compared to its progenitor *E. coli* BL21(DE3)ΔompA, *E. coli* BL21(DE3)Δ60 had similar growth kinetics, but released approximately 3-folds more OMVs (Figure 3b). OMVs from both strains were purified from the culture supernatants and their size and quality was analyzed by electron microscopy and light scattering using a Nanosight NS300 set with 532 nm laser. As shown in

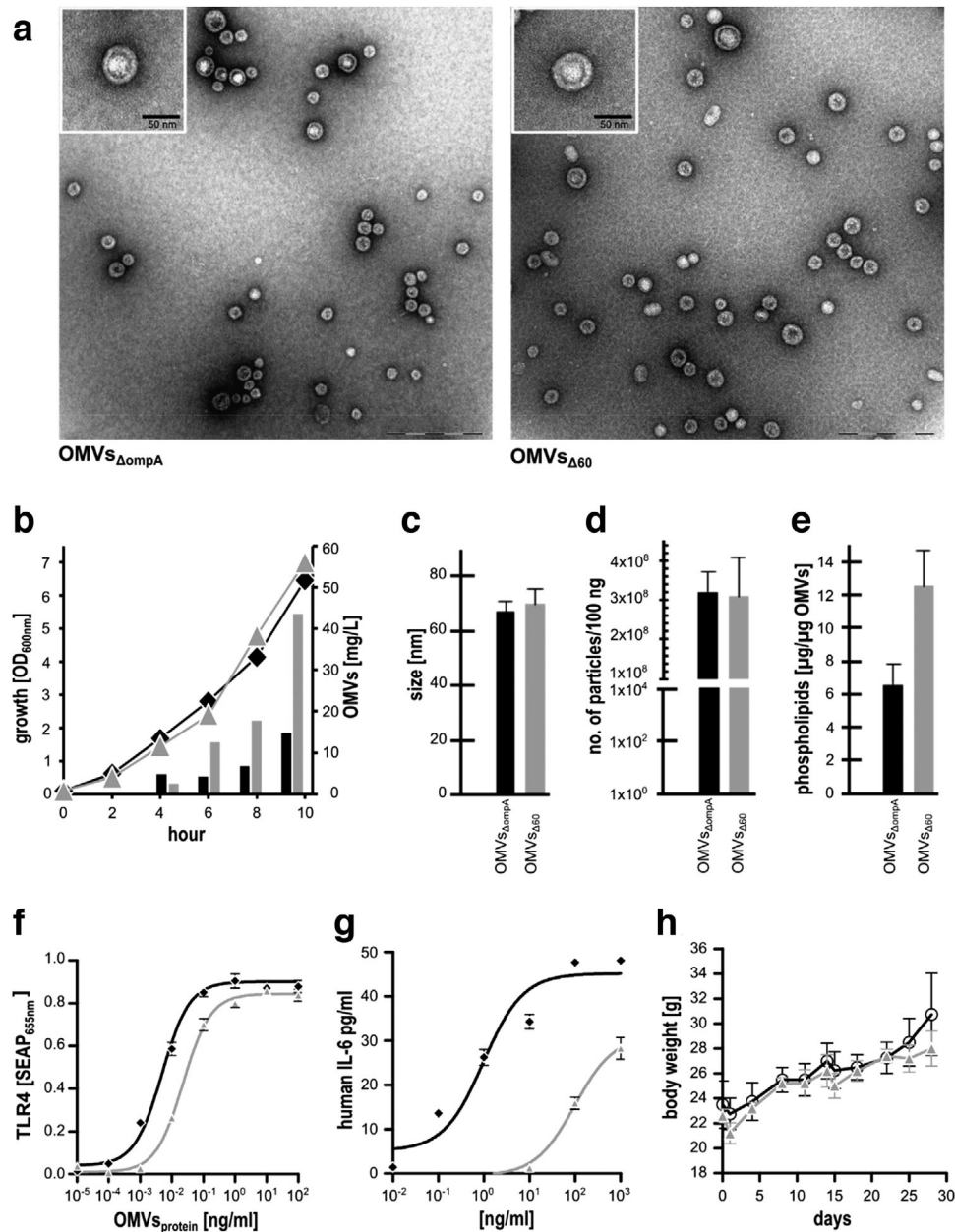


FIGURE 3 Properties of *E. coli* BL21(DE3) Δ 60 and OMVs $_{\Delta 60}$. (a) Morphology of OMVs $_{\Delta ompA}$ and OMVs $_{\Delta 60}$ analyzed by electron microscopy. (b) Comparison of growth kinetics and OMV productivity between *E. coli* BL21(DE3) Δ 60 and *E. coli* BL21(DE3) Δ ompA. *E. coli* BL21(DE3) Δ 60 (\blacktriangle) and *E. coli* BL21(DE3) Δ ompA (\blacklozenge) were grown in a bioreactor over a 10 h period and 50 ml cultures were collected at different time points and used for OMV purification and quantitation. OMVs productivity is given as mg/L (protein content). (c) Determination of OMV size - Purified OMVs were characterized using a Nanosight NS300. The size value is given as an average of two independent biological replicates, analyzed in duplicate. (d) Determination of particle number - OMVs were analyzed at a normalized concentration of 100 ng/ml and the number, determined using Nanosight NS300, represents the average value obtained from two OMV preparations and two independent analyses. (e) Determination of lipid content in OMVs - Styrylic membrane dye FM4-64 (Thermo Fisher Scientific, Waltham, MA USA) at a final concentration of 3.3 μ g/ml was added to 125 and 250 ng of OMVs. After 10 min at 37°C fluorescence was measured (excitation at 485 nm, emission at 670 nm) and lipid content was estimated as μ g/ μ g OMVs (protein based) using *E. coli* L- α -phosphatidylglycerol as standard. (f) Analysis of TLR4 agonistic activity of OMVs - HEK-Blue mTLR4 cells were incubated with different amounts of either OMVs $_{\Delta ompA}$ (\blacklozenge) or OMVs $_{\Delta 60}$ (\blacktriangle). After 17 h the levels of secreted alkaline phosphatase (SEAP) secreted upon mTLR4 stimulation by OMVs were determined by reading the absorbance of the culture supernatant at 655 nm in duplicate. (g) In vitro release of IL-6 by macrophages upon OMV stimulation - THP-1 human leukemic monocyte cells (4×10^5 cells in 10 μ L/well) differentiated to macrophages by PMA were incubated with different concentrations of OMVs $_{\Delta ompA}$ (\blacklozenge) and OMVs $_{\Delta 60}$ (\blacktriangle) in a final volume of 100 μ L/well. IL-6 release in the supernatants was measured by Human IL-6 Uncoated ELISA Kit (Thermo Fisher Scientific, Waltham, MA USA) in duplicate. (h) Body weight analysis of mice immunized with OMVs $_{\Delta 60}$ - Mice (5 mice/group) were immunized three times at 2-week intervals with 10 μ g of OMVs $_{\Delta 60}$ /dose in 100 μ L PBS containing 2 mg/ml of Alum hydroxide. Immunization with 100 μ L PBS containing 2 mg/ml of Alum hydroxide was used as control. Body weight of each mouse was measured at 3–5 day intervals over a period of 30 days. Curves are reported as average body weight ($n = 5$) of mice immunized with OMVs $_{\Delta 60}$ (\blacktriangle) or alum (\circ). Error bars in C-F and H: mean \pm s.d. Error bars in F and G: mean \pm s.e.m.

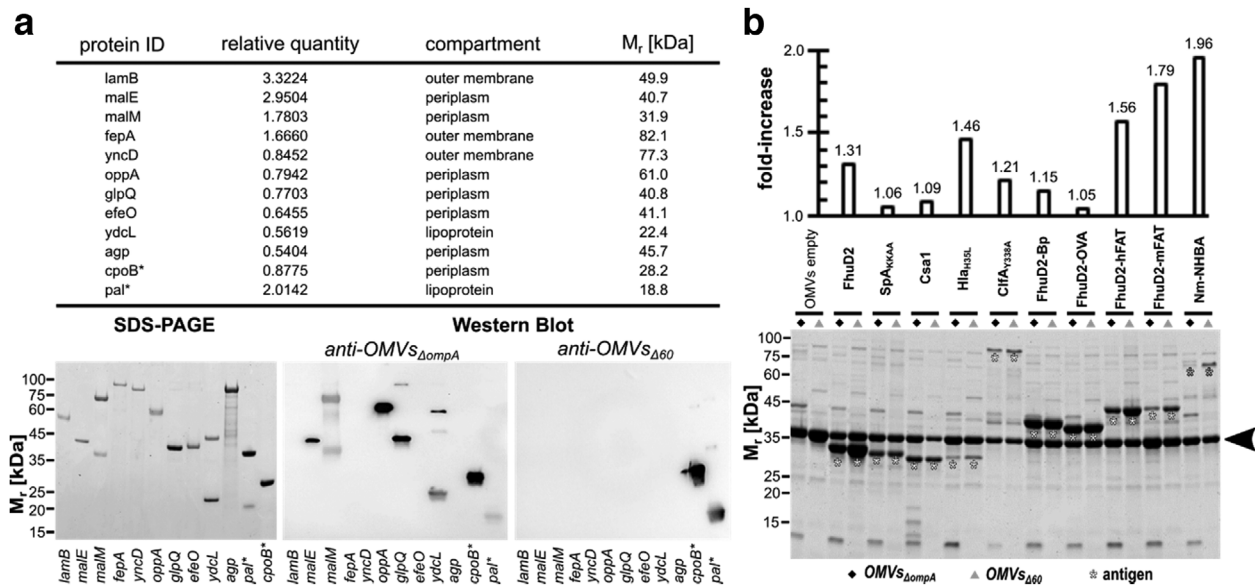


FIGURE 4 Immunogenicity of endogenous OMV proteins and expression of heterologous antigens in OMVs - (a) Ten proteins identified in OMVs_{ΔompA} by mass spectrometry were expressed as His-TAG fusions in *E. coli* BL21(DE3) and purified by IMAC. Purified proteins were analyzed by SDS-PAGE and Western Blot using sera from mice immunized with either OMVs_{ΔompA} or OMVs_{Δ60}. As a control, two proteins (*) present in both OMVs_{ΔompA} and OMVs_{Δ60} were also analyzed. Relative quantity refers to the number of pixel of the corresponding protein spot(s) in relation to the sum of pixel from all protein spots (= 100). (b) - *E. coli* BL21(DE3)ΔompA and *E. coli* BL21(DE3)Δ60 strains expressing different heterologous antigens as lipoproteins were grown in LB at 30°C. At OD₆₀₀ = 0.5, 0.1 mM IPTG was added and after 2 h OMVs were purified from culture supernatants by ultracentrifugation. Aliquots corresponding to 7.5 μg of total OMV proteins were loaded on each lane. The amount of recombinant antigens expressed in the OMVs was estimated by densitometry analysis of each lane using the formula: μg recombinant protein = μg OMVs × (pixels recombinant protein)/(total lane pixels). The upper panel indicates the ratio between the amount of each recombinant protein expressed in OMVs_{Δ60} and the amount of the same protein expressed in OMVs_{ΔompA} (see also Table S7). The arrowhead indicates the band corresponding to the most abundant protein (OmpF) in empty OMVs

Figure 3a, the size and the morphology of the vesicles from both samples looked very similar by electron microscopy, with no visible contamination or presence of aggregates. The similarity in size and number of vesicles/μg of total proteins of OMVs_{ΔompA} and OMVs_{Δ60} was confirmed by Nanosight analysis (Figure 3c, d), while the elimination of endogenous proteins (and probably the modification of the *mli* pathway) affected the phospholipid content, which was approximately twice as much in OMVs_{Δ60} with respect to OMVs_{ΔompA} (Figure 3e). In line with the inactivation of *msbB* and *pagP* genes, OMVs_{Δ60} had a TLR4 agonistic activity and IL-6 stimulation capacity approximately one and three orders of magnitude lower than OMVs_{ΔompA}, respectively (Figure 3f, g). These values appear to be in line with what reported for other OMV preparations for human use (Gerke et al., 2015; Ladhani et al., 2016; Rossi et al., 2016) and the safety profile of OMVs_{Δ60} was further confirmed by the absence of body weight loss in immunized mice (Figure 3h). Indeed, all OMVs_{Δ60} immunized mice experienced a ‘pain score’ 0/1, showing regular or slightly ruffled hair coat, healthy mucous membranes, normal physical activity and normal consumption of food and water. Considering that the 59 inactivated proteins include a number of lipoproteins, we also compared the TLR2 agonistic activity of OMVs_{Δ60} and OMVs_{ΔompA}. However, only a non-statistically significant decrease of TLR2 activation by OMVs_{Δ60} was observed (Fig. S3), suggesting that, in addition to lipoproteins, other OMV components can stimulate this innate immunity receptor.

One of the main motivations to create a strain releasing proteome-minimized OMVs was to reduce the immune responses toward OMV endogenous proteins and to enhance the immunogenicity of heterologous antigens. To test this, two proteins (the products of *cpoB* and *pal* genes) present in both OMVs_{Δ60} and OMVs_{ΔompA} and ten proteins only present in OMVs_{ΔompA}, were expressed in *E. coli*, purified and analyzed by Western Blot using sera from mice immunized with either OMVs_{Δ60} or OMVs_{ΔompA}. While CpoB and Pal proteins were stained by both sera, five out of the ten proteins absent in OMVs_{Δ60} were recognized only by the sera from OMVs_{ΔompA}-immunized mice (Figure 4a). Therefore, as expected, several OMVs endogenous proteins are immunogenic and their removal silenced the corresponding specific immune responses. To investigate whether the absence of some of OMV proteins could enhance the immune response toward the others, we separated the total proteins of OMVs_{ΔompA} and OMVs_{Δ60} on SDS-PAGE and we analyzed them by Western Blot using sera from mice immunized with either OMVs_{ΔompA} or OMVs_{Δ60}. As shown in Fig. S4, the anti-OMVs_{ΔompA} serum recognized a higher number of protein species in OMVs_{ΔompA} than in OMVs_{Δ60}. Moreover, no additional reactive proteins were observed in both OMVs_{ΔompA} and OMVs_{Δ60} using sera from mice immunized with OMVs_{Δ60}. Therefore, it appears that the poorly immunogenic proteins continue to remain so even if their relative abundance in OMVs would partially change as a result of the inactivation of others.

Finally, we asked the question whether the inactivation of endogenous proteins could affect the stability of OMVs. To test this we incubated the OMV preparations at different temperatures and we followed their stability over a period of three months using SDS-PAGE. No appreciable difference in the protein pattern could be detected even if OMVs were conserved at 37°C.

3.4 | Engineering of OMVs_{Δ60} with heterologous proteins

We next investigated whether the removal of the OMV endogenous proteins could have affected the loading capacity of OMVs. We previously showed that foreign antigens and epitopes efficiently compartmentalize in OMVs when their coding sequences are either directly fused to a lipoprotein leader sequence (Irene et al., 2019) or hooked to the C-terminus of an OMV-associated lipoprotein (Grandi et al., 2017, 2018). Therefore, we selected ten heterologous proteins and epitopes, we expressed them as lipidated antigens in both *E. coli* BL21(DE3) $\Delta ompA$ and *E. coli* BL21(DE3) $\Delta 60$ and we purified the vesicles from each recombinant strain. Purified vesicles were analyzed by SDS-PAGE and the amount of recombinant protein in each vesicle preparation was determined by densitometry analysis (Figure 4b). From these results, two main conclusions can be drawn. First, and in line with recently reported data (Irene et al., 2019), heterologous proteins efficiently compartmentalized in OMVs, where they could account for as much as 20%–30% of total OMVs proteins (Table S7). Second, the loading capacity of heterologous proteins was higher in OMVs_{Δ60} than OMVs_{ΔompA}, with an increase that could be as high as 90% (Figure 4b).

Finally, we asked the question whether the expression of heterologous antigens could have affected the stability of OMVs. To test this, we analyzed the OMV protein pattern after storing FhuD2-hFAT1-OMVs_{ΔompA} and of FhuD2-hFAT1-OMVs_{Δ58} at different temperatures (OMVs_{Δ58} derived from *E. coli* BL21(DE3) $\Delta 58$, a strain which differs from to *E. coli* BL21(DE3) $\Delta 60$ only for the absence of the *msbB* and *pagP* mutations. OMVs_{Δ58} have an identical proteome as OMVs_{Δ60}). Similarly to what observed with OMVs_{Δ60} and OMVs_{ΔompA}, the stability of the engineered OMVs was not impaired even after three-month incubation at 37°C.

3.5 | OMVs_{Δ60} as vaccine platform

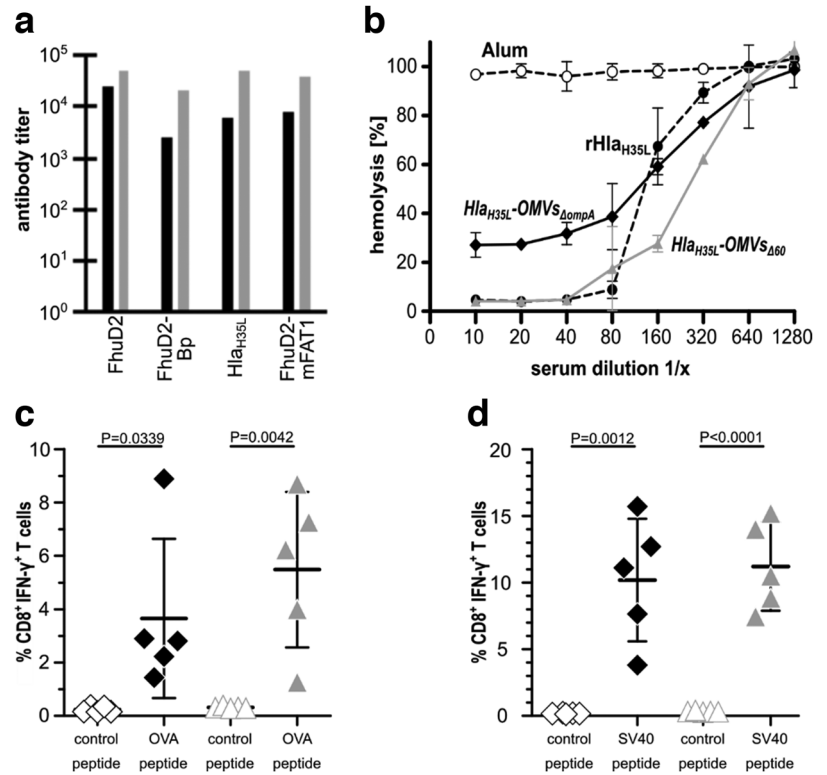
To test whether OMVs_{Δ60} decorated with heterologous antigens/epitopes could elicit antigen/epitope-specific immune responses, we selected four engineered OMVs_{Δ60} loaded with lipidated FhuD2, Hla_{H35L}, FhuD2-mFAT1 fusion and FhuD2-Bp fusion and we used them to immunize (i.p.) groups of BALB/c mice. FhuD2, Hla_{H35L} are two *S. aureus* protective antigens (Irene et al., 2019). FhuD2-mFAT1 is a C-terminal fusion carrying the murine homolog of a surface-exposed epitope of FAT1, a protein found overexpressed in colorectal cancer (Grandi et al., 2018; Pileri et al., 2016). Finally, FhuD2-Bp is a fusion carrying three copies of an immunogenic epitope (TRMQTQINGLNQGVSNAND) from *Burkholderia pseudomallei* flagellin separated by a short linker sequence (GS). After immunization, sera from animals of each group were pooled and antigen-specific antibody titers were measured by ELISA. High IgG titers were induced against all engineered antigens and in the case of the OMVs_{Δ60} decorated with Hla_{H35L}, FhuD2-mFAT1 and FhuD2-Bp the titers were approximately five to ten-fold higher than what obtained with animals immunized with engineered OMVs deriving from the progenitor *E. coli* BL21(DE3) $\Delta ompA$ strain (Figure 5a). The higher immunogenicity of engineered OMVs_{Δ60} was also confirmed by analyzing the ELISA titers of antigen-specific antibodies from single mouse sera. As shown in Fig.S6, sera from OMVs_{Δ60}-immunized mice had consistently higher levels of antigen-specific antibodies with respect to OMVs_{ΔompA}-immunized mice. Finally, in the case of Hla_{H35L}, we also determined the inhibition of Hla haemolytic activity of sera from mice immunized with engineered OMVs. Sera from mice immunized with Hla_{H35L}-OMVs_{Δ60} inhibited haemolysis at a three-fold higher dilution with respect to sera from Hla_{H35L}-OMVs_{ΔompA}-immunized mice (Figure 5b). Moreover, the anti-Hla_{H35L}-OMVs_{ΔompA} sera were not able to inhibit completely the Hla hemolytic activity, suggesting that the two sera differ in both quantitative and qualitative terms.

To be broadly applicable, OMVs should elicit not only humoral immunity but also cell-mediated immunity. Therefore, we tested the capacity of OMVs_{Δ60} to induce cytotoxic CD8⁺ T cell responses. To this aim, 5 μg of synthetic peptides corresponding to OVA and SV40 epitopes were absorbed to 10 μg of both OMVs_{ΔompA} and OMVs_{Δ60} and the OMV-peptide mixtures were used to immunize C57BL/6 mice. Animals were given two doses of vaccines, one week apart, and five days after the second immunization splenocytes were stimulated with the corresponding peptide and the frequency of IFN-γ-producing CD8⁺ T cells was determined by flow cytometry. Both immunizations elicited epitope-specific T cells at a frequency ranging from 3% to 15% of total splenocytic CD8⁺ T cells (Figure 5c, d). In particular, OMVs_{Δ60} had a tendency to elicit higher frequencies of T cells even though, for a rigorous statistical analysis, a higher number of animals should be used.

4 | DISCUSSION

In this work, we have described the creation of an *E. coli* derivative, *E. coli* BL21(DE3) $\Delta 60$, in which 60 genes have been inactivated using a highly efficient CRISPR/Cas9-based genome editing approach. The strain features the release of OMVs deprived of

FIGURE 5 Immunogenicity and functional immune responses in mice immunized with OMVs_{Δ60} decorated with heterologous antigens/epitopes – (a) IgG titers in mice immunized with OMVs decorated with lipidated heterologous antigens. Groups of five female BALB/c mice were immunized i.p. 3 times at two-week intervals with 2 μg of engineered OMVs_{ΔompA} (black bars) and OMVs_{Δ60} (grey bars) in Alum. Sera were collected 7 days after the third immunization and IgG titers were measured in triplicate by ELISA, coating the plates (200 ng/well) with either the corresponding purified recombinant antigen (FhuD2 and Hla_{H35L}) or the corresponding synthetic peptide (Bp and mFAT1). (b) Functional activity of anti-HLA antibodies elicited by Hla_{H35L}-OMVs_{Δ60} – Purified Hla was incubated with rabbit erythrocytes in the presence or absence of different dilutions of sera from mice immunized with Hla_{H35L}-OMVs_{Δ60}, Hla_{H35L}-OMVs_{ΔompA}, or purified recombinant Hla_{H35L} (10 μg) in Alum. Inhibition of Hla hemolytic activity is given as percentage of hemolytic activity obtained incubating the rabbit erythrocytes with water. Error bars: mean ± s.d. (c and d) Analysis of epitope-specific CD8⁺ T cells elicited by immunization with OMVs absorbed with synthetic peptides corresponding to OVA and SV40 CD8⁺ T cell epitopes – C57BL/6 mice (5 animals/group) were immunized with 10 μg of OMVs_{ΔompA} or OMVs_{Δ60} ‘absorbed’ to 5 μg of either OVA peptide or SV40 peptide. After 5 days, splenocytes were collected from each animal and peptide-specific IFN-γ producing CD8⁺ T cells were counted by flow cytometry, after stimulation with the specific peptide (OMVs_{ΔompA} ◆ and OMVs_{Δ60} ▲) or an irrelevant peptide (open symbols). Error bars: mean ± s.e.m.



59 endogenous proteins and carrying a penta-acylated lipopolysaccharide. We also describe the main properties of the OMVs released by *E. coli* BL21(DE3)Δ60 and how the strain can be exploited for the development of effective OMV-based vaccines.

We believe that this work delivers a number of messages that can be of interest from technological, scientific and translational standpoints.

From a technical standpoint, we validated our CRISPR/Cas9-based gene editing approach (Zerbini et al., 2017), which demonstrated that sequential, multiple gene manipulations could be accumulated in the same strain at a pace of one mutation every other day. With the present work, once the 90 genes were selected, it took us approximately one month to produce the corresponding 90 pCRISPR-SacB-gDNA plasmids and double stranded donor DNAs, and we completed the whole process of sequential gene knockouts in roughly 1 year (approximately two mutations/working week). Considering that our protocol allows the efficient simultaneous introduction of at least two mutations at a time, strains carrying selective gene modifications could theoretically be accelerated to a pace of four mutations/week.

From a scientific standpoint, we believe that our work offers a collection of data, which might be useful to better understand the role of specific gene products and the complex network of protein-protein interactions occurring in the periplasmic and outer membrane compartments. As stated above, all genes selected for this study were classified as ‘dispensable’ (Baba et al., 2006) and could be singularly inactivated without affecting viability (Zerbini et al., 2017). The fact that some combinations of gene deletions appeared to be not compatible (or at least were not selected using the screening procedure adopted in our protocol) opens the question as to which relationship these genes have with the others to make their deletion incompatible with survival under the growth conditions used. Addressing this question could be of particular interest for those genes whose encoded proteins are still classified as ‘hypothetical and/or unknown’. If we look at the network connecting all selected 90 genes as it emerges from STRING database (Szklarczyk et al., 2019), it appears that most of the ‘non-permissive’ mutations fall in those genes/gene products that have some physical (i.e. transcriptional) or functional association with others (‘red nodes’ in Figure 6). One possible explanation is that at least some of the genes exert important redundant functions. For instance, *yncE*, a gene with unknown function, is connected with a number of genes (*fhuA*, *fepA*, *cirA*, *yncD*, *fecA*) all involved in iron metabolism/transport. Therefore, the simultaneous deletion of all six genes could impair iron assimilation to a non-permissible level. Interestingly, five of the non-permissive mutations, *mdoG*, *potD*, *kpsD*, *yifL* and *ppiA*, include genes that seem to have no relationship with any others (‘yellow dots’ in Figure 6). Such observation deserves further investigation.

Another interesting result from our study is that the removal of proteins did not substantially affect size and number of OMVs, as estimated after normalization to protein content (Figure 3c, d) and by electron microscopy analysis (Figure 3a). This could

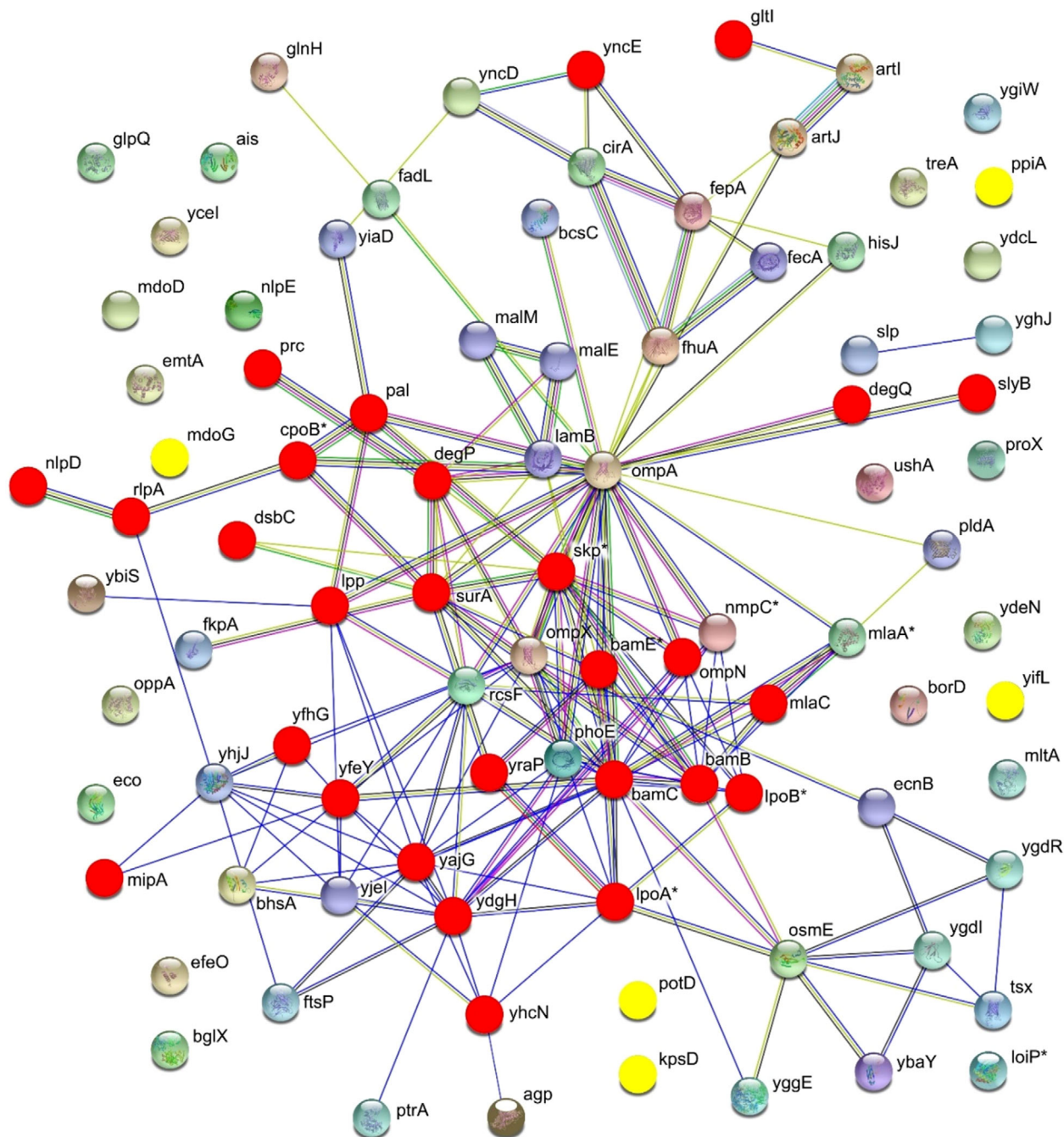


FIGURE 6 Physical and functional network among the 90 genes selected for gene knockout - The 90 genes selected for gene knockout (Figure 1) were analyzed together with *ompA* using STRING database to visualize their possible physical (i.e. transcriptional) and functional association. Lines indicate which genes the database considers correlated according to different criteria and the number of connecting lines correlates with the number of association criteria. Red and yellow dots represent the genes whose inactivation failed or resulted in impaired growth and/or OMV productivity (see Discussion for more explanation). Asterisks indicate those proteins for which the STRING database has assigned different synonymous names with respect to those used in Figure 1 (see Table S1)

be explained assuming that OMVs carry a constant protein cargo and the loss of one protein species tends to be compensated with the accumulation of some others. This effect can be appreciated in Figure 4b: the intensity of the abundant OmpF band is higher in $OMVs_{\Delta 60}$ than $OMVs_{\Delta ompA}$ (lanes 1 and 2) and the accumulation of heterologous proteins parallels the reduction of other bands, predominantly OmpF. While size and number of vesicles/ μg of protein remain unchanged, phospholipid content is higher in $OMVs_{\Delta 60}$ (Figure 3e). This difference could be due to the structural modification of Lipid A between $OMVs_{\Delta 60}$ and $OMVs_{\Delta ompA}$. The absence of an acyl moiety might either affect the phospholipid determination or be compensated by the additional transport of phospholipids in the external leaflet of the outer membrane. Moreover, phospholipid accumulation is physiologically regulated by an ABC transport system, comprising a number of genes involved in the maintenance of

OM lipid asymmetry (*mfa* pathway) (Malinverni & Silhavy, 2009). It is likely that the inactivation of *mfaA* in *E. coli* BL21(DE3) Δ 60 contributes to the increase of phospholipid content in OMVs Δ 60 and to the hyper-vesiculating phenotype, similarly to what observed in *Haemophilus influenzae*, *Vibrio cholerae* and *E. coli* (Kulp et al., 2015; Roier et al., 2016).

From a translational standpoint, we believe that *E. coli* BL21(DE3) Δ 60 can find concrete applications in vaccine development. As already pointed out, OMVs are becoming an attractive vaccine platform, but require optimization for a broad application. This study represents an important step forward in this regard. Essentially, *E. coli* BL21(DE3) Δ 60 releases vesicles with several important properties. First, the strain produces > 40 mg/L of vesicles (protein based) under the laboratory conditions we used. Such yield, which can surely be further optimized in large-scale production processes, is nonetheless sufficient to guarantee the formulation of approximately 1,000 vaccine doses/L, assuming a 25–50 μ g OMVs/dose for human applications. Second, we have shown that the elimination of 59 OMV endogenous proteins has a beneficial effect on the level of expression and immunogenicity of heterologous antigens. Recombinant proteins can be incorporated into OMVs at a level consistently higher (up to 90%) compared to the progenitor strain. Moreover, in most of the cases we analysed, antigen-specific antibody titres elicited by engineered OMVs Δ 60 were superior to what obtained with OMVs Δ ompA. This could be a consequence of the higher antigen expression level or of the absence of the 59 endogenous proteins, which could otherwise interfere with, or dilute the antigen-specific immune responses. Indeed, we showed that many endogenous proteins are immunogenic in the mouse model and therefore their removal should be beneficial for an optimal immune response against heterologous antigens, as demonstrated for a number of antigen, including Hla_{H35L} (Figure 5a, b).

Immune responses elicited by OMVs Δ 60 are not restricted to antibodies. Our data show that when formulated with two CD8⁺ T cell synthetic epitopes elevated frequencies of epitope-specific CD8⁺ T cells were induced in immunized mice, with frequencies ranging from 3% to 8% and 7% to 15% in the case of OVA and SV40 epitopes, respectively. In our hands, other adjuvants already used in humans, such as CpG and Hiltonol, did not promote such elevated epitope-specific CD8⁺ T cell frequencies. Considering the importance of T cell responses in cancer immunotherapy, our data suggest that OMVs Δ 60 can be exploited not only as ingredient for infectious disease vaccines but also for cancer vaccines.

Moreover, we showed that OMVs Δ 60 have a safety profile similar if not superior to what reported for the OMV vaccines already in clinical use (Gerke et al., 2015; Rossi et al., 2016), an important feature in view of their future human applications.

Finally, the OMV stability appears to be particularly striking. Although stability studies using different OMV preparations are still in progress, prolonged conservation of our vesicles even at room temperature does not modify their overall protein profile, and this is true for both OMVs Δ ompA and OMVs Δ 60 as well as for the engineered OMVs analyzed so far. We are collecting 1-year stability data on different OMV preparations and the results so far available confirm the robustness of the preparations. High stability is a remarkable property of our OMVs also in view of their application in developing countries where it would be difficult to guarantee a cold chain for temperature-sensitive formulations.

Taking into account all advantageous characteristics presented here, we believe that *E. coli* BL21(DE3) Δ 60 has the potential to become a workhorse factory for novel OMV-based vaccines.

ACKNOWLEDGEMENTS

We thank Prof. M. Bolognesi (University of Milan, Italy), Prof. G. Colombo (University of Pavia, Italy) and Dr. L. Gourlay (University of Milan, Italy), collaborators of the PRIN-2015 project, for providing *Burkholderia pseudomallei* epitope sequence and purified protein for immunogenicity studies. The authors wish to thank NGS Facility as well as Federica Armanini and Francesco Beghini (University of Trento, Italy) for library preparation, sequencing and data analysis. Furthermore, we gratefully thank the Department facilities for their technical support, in particular Sergio Robbiati (animal facility), Cristina Del Bianco (protein facility) and Isabella Pesce (cell analysis and separation facility). We are grateful to Alessandro Armini (University of Siena) for his assistance in the identification of protein spots.

Most of this work has been financially supported by the Advanced European Research Council grant OMVAC 340915 and partially supported by National Funding PRIN-2015 (CUPE62F16001630001) (both assigned to Guido Grandi).

AUTHOR CONTRIBUTIONS

Guido Grandi conceived and designed the study, analyzed data and wrote the manuscript; Yaqoub Ashhab coordinated the bioinformatics analysis; Ilaria Zanella, Enrico König and Francesca Zerbini performed knockouts; Carmela Irene, Michele Tomasi, Riccardo Corbellari, Alberto Grandi: OMV engineering; Ilaria Zanella, Enrico König, Michele Tomasi, Luca Frattini, Laura Fantappiè, Carmela Irene, Riccardo Corbellari, Samine J. Isaac, Martina Grigolato, and Alberto Grandi: OMV production and purification; Enrico König, Luca Frattini, Michele Tomasi, Assunta Gagliardi and Alberto Grandi: biochemical and biophysical characterization of OMVs; Michele Tomasi, Ilaria Zanella, Enrico König and Alberto Grandi: OMV immunogenicity; Michele Tomasi, Laura Fantappiè, Silvia Valensin, Samine J. Isaac and Martina Grigolato: mouse models; Ilaria Zanella, Assunta Gagliardi and Elena Caproni: *in vitro* assays; Enrico König and Carmela Irene: recombinant protein purification; Assunta Gagliardi and Luca Bini: 2-DE and MS analysis; Ilaria Ferlenghi and Fabiola Giusti electron microscopy analysis; Enrico König edited manuscript, Tables and Figures and all authors read, corrected and approved the final manuscript.

CONFLICTS OF INTEREST

Guido Grandi, Alberto Grandi, Enrico König, Ilaria Zanella, Laura Fantappiè and Carmela Irene are co-inventors of patents on OMVs; Alberto Grandi and Guido Grandi are involved in a biotech company interested in exploiting the OMV platform.

ORCID

Enrico König  <https://orcid.org/0000-0002-1560-5948>

REFERENCES

- Altschul, S. F., Gish, W., Miller, W., Myers, E. W., & Lipman, D. J. (1990). Basic local alignment search tool. *Journal of Molecular Biology* 215, 403–410
- Baba, T., Ara, T., Hasegawa, M., Takai, Y., Okumura, Y., Baba, M., Datsenko, K. A., Tomita, M., Wanner, B. L., & Mori, H. (2006). Construction of Escherichia coli K-12 in-frame, single-gene knockout mutants: The Keio collection. *Molecular Systems Biology* 2, 1–11
- Baumans, V., Brain, P. F., Brugère, H., Clausing, P., Jeneskog, T., & Perretta, G. (1994). Pain and distress in laboratory rodents and lagomorphs. *Laboratory Animals* 28, 97–112
- Berlanda Scorza, F., Colucci, A. M., Maggiore, L., Sanzone, S., Rossi, O., Ferlenghi, I., Pesce, I., Caboni, M., Norais, N., Di Cioccio, V., Saul, A., & Gerke, C. (2012). High yield production process for Shigella outer membrane particles. *PLoS One* 7, e35616.
- Bishop, D. G., & Work, E. (1965). An extracellular glycolipid produced by Escherichia coli grown under lysine-limiting conditions. *The Biochemical Journal* 96, 567–576
- Chatterjee, S. N., & Das, J. (1967). Electron microscopic observations on the excretion of cell-wall material by Vibrio cholerae. *Journal of General Microbiology* 49, 1–11
- Chen, D. J., Osterrieder, N., Metzger, S. M., Buckles, E., Doody, A. M., Delisa, M. P., & Putnam, D. (2010). Delivery of foreign antigens by engineered outer membrane vesicle vaccines. *Proceedings of the National Academy of Sciences of the United States of America* 107, 3099–3104
- Ellis, T. N., & Kuehn, M. J. (2010). Virulence and immunomodulatory roles of bacterial outer membrane vesicles. *Microbiol. Molecular Biology Reviews* 74, 81–94
- Fantappiè, L., Irene, C., De Santis, M., Armini, A., Gagliardi, A., Tomasi, M., Parri, M., Cafardi, V., Bonomi, S., Ganfani, L., Zerbini, F., Zanella, I., Carnemolla, C., Bini, L., Grandi, A., & Grandi, G. (2017). Some Gram-negative lipoproteins keep their surface topology when transplanted from one species to another and deliver foreign polypeptides to the bacterial surface. *Molecular & Cellular Proteomics : MCP* 16, 1348–1364
- Gagliardi, A., Lamboglia, E., Bianchi, L., Landi, C., Armini, A., Ciolfi, S., Bini, L., & Marri, L. (2016). Proteomics analysis of a long-term survival strain of Escherichia coli K-12 exhibiting a growth advantage in stationary-phase (GASP) phenotype. *Proteomics* 16, 963–972
- Gerke, C., Colucci, A. M., Giannelli, C., Sanzone, S., Vitali, C. G., Sollai, L., Rossi, O., Martin, L. B., Auerbach, J., Di Cioccio, V., & Saul, A. (2015). Production of a Shigella sonnei vaccine based on generalized modules for membrane antigens (GMMA), 1790GAHB. *PLoS One* 10, e0134478.
- Gerritzen, M. J.H., Martens, D. E., Wijffels, R. H., Van Der Pol, L., & Stork, M. (2017). Bioengineering bacterial outer membrane vesicles as vaccine platform. *Biotechnology Advances* 35, 565–574
- Grandi, A., Fantappiè, L., Irene, C., Valensin, S., Tomasi, M., Stupia, S., Corbellari, R., Caproni, E., Zanella, I., Isaac, S. J., Ganfani, L., Frattini, L., König, E., Gagliardi, A., Tavarini, S., Sammiceli, C., Parri, M., & Grandi, G. (2018). Vaccination with a FAT1-derived B cell epitope combined with tumor-specific B and T cell epitopes elicits additive protection in cancer mouse models. *Frontiers in Oncology* 8, 481
- Grandi, A., Tomasi, M., Zanella, I., Ganfani, L., Caproni, E., Fantappiè, L., Irene, C., Frattini, L., Isaac, S. J., König, E., Zerbini, F., Tavarini, S., Sammiceli, C., Giusti, F., Ferlenghi, I., Parri, M., & Grandi, G. (2017). Synergistic protective activity of tumor-specific epitopes engineered in bacterial Outer Membrane Vesicles. *Frontiers in Oncology* 7, 1–12
- Hisham, Y., & Ashhab, Y. (2018). Identification of cross-protective potential antigens against pathogenic Brucella spp. through combining pan-genome analysis with reverse vaccinology. *Journal of Immunology Research* 2018, 1.
- Irene, C., Fantappiè, L., Caproni, E., Zerbini, F., Anesi, A., Tomasi, M., Zanella, I., Stupia, S., Prete, S., Valensin, S., König, E., Frattini, L., Gagliardi, A., Isaac, S. J., Grandi, A., Guella, G., & Grandi, G. (2019). Bacterial outer membrane vesicles engineered with lipidated antigens as a platform for Staphylococcus aureus vaccine. *Proceedings of the National Academy of Sciences of the United States of America* 116, 21780–21788
- Kaparakis-Liaskos, M., & Ferrero, R. L. (2015). Immune modulation by bacterial outer membrane vesicles. *Nature Reviews. Immunology* 15, 375–387
- Keseler, I. M., Mackie, A., Santos-Zavaleta, A., Billington, R., Bonavides-Martínez, C., Caspi, R., Fulcher, C., Gama-Castro, S., Kothari, A., Krummenacker, M., Latendresse, M., Muñoz-Rascado, L., Ong, Q., Paley, S., Peralta-Gil, M., Subhraveti, P., Velázquez-Ramírez, D. A., Weaver, D., Collado-Vides, J., ... Karp, P. D. (2017). The EcoCyc database: Reflecting new knowledge about Escherichia coli K-12. *Nucleic Acids Research*. 45, D543–D550
- Kesty, N. C., & Kuehn, M. J. (2004). Incorporation of heterologous outer membrane and periplasmic proteins into Escherichia coli Outer Membrane Vesicles. *The Journal of Biological Chemistry* 279, 2069–2076
- Klock, H. E., & Lesley, S. A. (2009). The Polymerase Incomplete Primer Extension (PIPE) method applied to high-throughput cloning and site-directed mutagenesis. *Methods in Molecular Biology (Clifton, N.J.)* 498, 91–103
- Kulp, A. J., Sun, Bo, Ai, T., Manning, A. J., Orench-Rivera, N., Schmid, A. K., & Kuehn, M. J. (2015). Genome-wide assessment of outer membrane vesicle production in Escherichia coli. *PLoS One* 10, e0139200.
- Kulp, A., & Kuehn, M. J. (2010). Biological functions and biogenesis of secreted bacterial outer membrane vesicles. *Annual Review of Microbiology* 64, 163–184
- Ladhani, S. N., Ramsay, M., Borrow, R., Riordan, A., Watson, J. M., & Pollard, A. J. (2016). Enter B and W: Two new meningococcal vaccine programmes launched. *Archives of Disease in Childhood* 101, 91–95
- Malinverni, J. C., & Silhavy, T. J. (2009). An ABC transport system that maintains lipid asymmetry in the Gram-negative outer membrane. *Proceedings of the National Academy of Sciences of the United States of America* 106, 8009–8014
- Parikh, S. R., Andrews, N. J., Beebejaun, K., Campbell, H., Ribeiro, S., Ward, C., White, J. M., Borrow, R., Ramsay, M. E., & Ladhani, S. N. (2016). Effectiveness and impact of a reduced infant schedule of 4CMenB vaccine against group B meningococcal disease in England: A national observational cohort study. *Lancet* 388, 2775–2782
- Pileri, P., Campagnoli, S., Grandi, A., Parri, M., De Camilli, E., Song, C., Ganfani, L., Lacombe, A., Naldi, I., Sarmientos, P., Cinti, C., Jin, B., Grandi, G., Viale, G., Terracciano, L., & Grifantini, R. (2016). FAT1: A potential target for monoclonal antibody therapy in colon cancer. *British Journal of Cancer* 115, 40–51
- Roier, S., Zingl, F. G., Cakar, F., Durakovic, S., Kohl, P., Eichmann, T. O., Klug, L., Gadermaier, B., Weinzerl, K., Prassl, R., Lass, A., Daum, G., Reidl, J., Feldman, M. F., & Schild, S. (2016). A novel mechanism for the biogenesis of outer membrane vesicles in Gram-negative bacteria. *Nature Communications* 7, 10515.

- Rossi, O., Caboni, M., Negrea, A., Necchi, F., Alfini, R., Micoli, F., Saul, A., Maclennan, C. A., Rondini, S., & Gerke, C. (2016). Toll-Like receptor activation by generalized modules for membrane antigens from Lipid A mutants of *Salmonella enterica* Serovars Typhimurium and Enteritidis. *Clinical and Vaccine Immunology: CVI* 23, 304–314
- Serruto, D., Bottomley, M. J., Ram, S., Giuliani, M. M., & Rappuoli, R. (2012). The new multicomponent vaccine against meningococcal serogroup B, 4CMenB: Immunological, functional and structural characterization of the antigens. *Vaccine* 30, B87–B97.
- Somerville, J. E., Cassiano, L., Bainbridge, B., Cunningham, M. D., & Darveau, R. P. (1996). A novel *Escherichia coli* lipid A mutant that produces an antiinflammatory lipopolysaccharide. *The Journal of Clinical Investigation* 97, 359–365
- Szklarczyk, D., Gable, A. L., Lyon, D., Junge, A., Wyder, S., Huerta-Cepas, J., Simonovic, M., Doncheva, N. T., Morris, J. H., Bork, P., Jensen, L. J., & Mering, C. V. (2019). STRING v11: Protein-protein association networks with increased coverage, supporting functional discovery in genome-wide experimental datasets. *Nucleic Acids Research*. 47, D607–D613
- Van Der Pol, L., Stork, M., & Van Der Ley, P. (2015). Outer membrane vesicles as platform vaccine technology. *Biotechnology Journal* 10, 1689–1706
- Vorachek-Warren, M. K., Ramirez, S., Cotter, R. J., & Raetz, C. R.H. (2002). A triple mutant of *Escherichia coli* lacking secondary acyl chains on lipid A. *The Journal of Biological Chemistry* 277, 14194–14205
- Zerbini, F., Zanella, I., Fraccascia, D., König, E., Irene, C., Frattini, L F, Tomasi, M., Fantappiè, L., Ganfini, L., Caproni, E., Parri, M., Grandi, A., & Grandi, G. (2017). Large scale validation of an efficient CRISPR/Cas-based multi gene editing protocol in *Escherichia coli*. *Microbial Cell Factories* 16, 1–18

SUPPORTING INFORMATION

Additional supporting information may be found online in the Supporting Information section at the end of the article.

How to cite this article: Zanella I, König E, Tomasi M, et al. Proteome-minimized outer membrane vesicles from *Escherichia coli* as a generalized vaccine platform. *J Extracell Vesicles*. 2021;10:e12066. <https://doi.org/10.1002/jev2.12066>